Biophysical Chemistry 14 (1981) 1–9
Elsevier/North-Holland Biomedical Press

POLARIZATION OF THE ION ATMOSPHERE OF A CHARGED CYLINDER

Donald C. RAU and Elliot CHARNEY

Laboratory of Chemical Physics, National Institute of Arthritis, Metabolism and Digestive Diseases, National Institutes of Health, Bethesda, MD 20205, U.S.A.

Received 18 September 1980

The dipole moment is calculated for an electric-field-induced polarization of a Debye–Hückel ion atmosphere surrounding a charged rod. If L is the length of a thin rod, Q is its linear charge density, Z is charge of the salt ion in solution, and κ is the Debye–Hückel shielding parameter, then for $\kappa L \lesssim 10$, the calculated polarizability is proportional to $Z^2Q^2L^{1.8}/\kappa^{1.2}$. Comparison with experimental data for DNA shows that the ion atmosphere dipole is of the correct magnitude and is consistent with observed variations with Z, Q, L and κ.

1. Introduction

In the absence of a permanent dipole moment, the axial polarizability of a uniformly charged, rod-like polyion is responsible for its dielectric properties and orientation by electric fields. The sources of this polarizability reside in the distortion of the neutral valence structure and in the field-induced anisotropy of the surrounding counterions relative to the intrinsic polyion charge distribution. One such polyion under investigation is DNA. Experimentally, it is observed that the induced dipole of DNA is inversely dependent on the ionic strength of the solution [1–3]. Most theoretical treatments [3–6] have dealt with the field-induced polarization of counterions that are closely associated with or bound to DNA. In order to explain the observed dependence on ionic strength, it must be assumed that the number of bound counterions is significantly dependent on the concentration of free counterions. In recent years, however, the highly charged nature of DNA has prompted the development of the very successful counterion condensation theory by Manning [7]. To briefly summarize, counterions are divided into two classes. There is a layer of condensed or bound counterions on the DNA surface that neutralize most of the phosphate charge. The effective charge density varies with the inverse of the counterion charge. Surrounding this layer is a more diffuse ion atmosphere that can be treated in the familiar Debye–Hückel approximation. Importantly, it is expected on the basis of this work that the number of condensed counterions is only slightly dependent on the free counterion concentration. Working within the condensed counterion framework, Manning [8] and Charney et al. [9] have developed expressions for the polarizability of the condensed layer and found that the induced dipole should only weakly depend on the ionic strength and in the opposite direction to that found experimentally. The calculated polarizabilities, however, are of the correct magnitude.

Another possible source of dipole energy is through a field-induced polarization of the ion atmosphere. It is the purpose of this paper to calculate the polarizability of a Debye–Hückel ion atmosphere surrounding a charged rod. It will be shown that over the range of ionic strengths and rod lengths commonly used, the predicted polarizability is approximately proportional to the inverse square root of the ionic strength (proportional to the screening length, $1/\kappa$) and to the square of the rod length. When there is only one charge type of counterion, the treatment gives a result equivalent to "condensation theory", the the polarizability is not dependent on the effective DNA charge density.

2. Theory

The particular model we shall consider is illustrated in fig. 1. An insulating, impenetrable rod of radius a' is oriented parallel with respect to an applied electric field of magnitude E'. The rod is uniformly charged over a length $2L'$ centered on the origin, to a constant linear charge density Q. Surrounding this central rod is a simple $Z-Z$ electrolyte solution, characterized by a number concentration of cations or anions, n_0, and a bulk dielectric constant ϵ. In order to avoid troublesome boundary conditions at the endplates, we shall consider the rod to be infinitely long, but only charged over a length $2L'$. The effect of this will be negligible if $\kappa a' < 1$, where κ is the Debye–Hückel shielding parameter and is defined by

$$\kappa^2 = 8\pi Z^2 e^2 n_0/\epsilon kT. \tag{1}$$

At the low ionic strengths commonly used for electric dichroism and birefringence measurements, $\kappa a'$ is sufficiently small for DNA such that neglecting the endplates is justifiable.

In calculating the dipole energy from polarization of the ion atmosphere, we shall only consider electrostatic and diffusive forces, i.e. hydrodynamic interactions between moving charges will be neglected. The cylindrical coordinate system of the rod is the one we shall use, with distances parallel to the rod being x and distances normal to the rod being r.

We define the concentration distribution functions for cations and anions, $n_+(x,r)$ and $n_-(x,r)$, in terms of the dimensionless functions, $\nu_+(r,x)$ and $\nu_-(r,x)$, as

$$n_+(x,r) = n_0[1+\nu_+(x,r)], \qquad n_-(x,r) = n_0[1+\nu_-(x,r)]. \tag{2}$$

Additionally, if we let $\psi(r,x)$ be the electrostatic potential due to the distribution of charges in solution and let $-E'x$ be the applied electric potential, then at steady-state flow we have [10,11]

$$-(Ze/kT)\nabla\cdot[(1+\nu_+)\nabla(\psi'-E'x)] - \nabla^2\nu_+ = 0. \tag{3}$$

$$(Ze/kT)\nabla\cdot[(1+\nu_-)\nabla(\psi'-E'x)] - \nabla^2\nu_- = 0. \tag{4}$$

The potential ψ' is related to ν_+ and ν_- by the Poisson equation

$$\nabla^2\psi' = -(4\pi Zen_0/\epsilon)(\nu_+ - \nu_-). \tag{5}$$

It should be mentioned again that eqs. (3) and (4) neglect all hydrodynamic interactions between charges.

For large r, it is assumed that the influence of the central rod vanishes, or that

$$\lim_{r\to\infty} (\nu_+, \nu_-, \text{and } \psi') = 0. \tag{6}$$

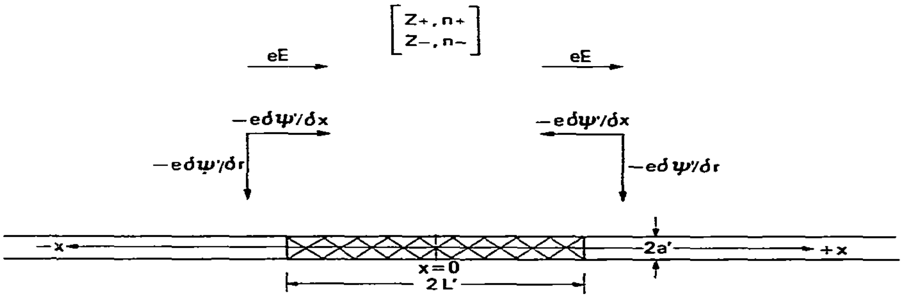

Fig. 1. A schematic representation of the model we consider in calculating the polarizability of a Debye–Hückel ion atmosphere surrounding a charged rod. The dimensions of the rod and solution composition are explained in the text. The arrows show the directions of the electrostatic forces from the applied field, E, and a negative charged rod on a positive test charge in the solution.

At the surface of the rod ($r=a'$), the boundary condition for the potential is the standard gaussian relationship

$$\begin{aligned} \partial\psi'/\partial r|_{a'} &= -2ZQ/\epsilon a', && \text{for } |x|\leqslant L', \\ &=0, && \text{for } |x|>L'. \end{aligned} \tag{7}$$

Since the rod is assumed impenetrable, the radial velocities for cations and anions must vanish at the surface, or

$$\partial\nu_+/\partial r|_{a'} + (Ze/kT)[1+\nu_+(a',x)]\partial\psi'/\partial r|_{a'} = 0, \quad \text{all } x, \tag{8}$$

$$\partial\nu_-/\partial r|_{a'} - (Ze/kT)[1+\nu_-(a',x)]\partial\psi'/\partial r|_{a'} = 0, \quad \text{all } x. \tag{9}$$

These are then the equations and associated boundary conditions that must be solved in order to determine the ion atmosphere polarization. In terms of the above functions, the dipole moment, m, due to the ion atmosphere is given by

$$m = 2\pi Zen_0 \int_{-\infty}^{+\infty} x\,\mathrm{d}x \int_{a'}^{\infty} r\,\mathrm{d}r[\nu_+(x,r)-\nu_-(x,r)], \tag{10}$$

where $\nu_+ - \nu_-$ represents a reduced charge density in a small volume of the ion atmosphere.

At this point it is convenient to recast the equations in terms of the functions,

$$\begin{aligned} &f(x,r)=\nu_+(x,r)-\nu_-(x,r), \qquad g(x,r)=\nu_+(x,r)+\nu_-(x,r), \\ &Ex=ZeE'(\kappa x)/\kappa kT, \qquad \psi=(Ze/kT)\psi'. \end{aligned} \tag{11}$$

Additionally, we can transform x and r to the dimensionless distances y and ρ by

$$y=\kappa x, \qquad \rho=\kappa r, \tag{12}$$

where κ is defined in eq. (1). In terms of these new parameters, eqs. (3)–(5) now take the form

$$\nabla^2 f - f = E\,\partial g/\partial y + \tfrac{1}{2}gf - \nabla g\cdot\nabla\psi, \tag{13}$$

$$\nabla^2 g = E\,\partial f/\partial y + \tfrac{1}{2}f^2 - \nabla f\cdot\nabla\psi, \tag{14}$$

$$\nabla^2\psi = -\tfrac{1}{2}f, \tag{15}$$

where the gradient ∇ is in terms of the reduced parameters y and ρ, and the laplacian, ∇^2, in cylindrical coordinates has the form

$$\nabla^2 = \partial^2/\partial\rho^2 + \rho^{-1}\,\partial/\partial\rho + \partial^2/\partial y^2. \tag{16}$$

The boundary conditions, eqs. (6)–(9) become

$$\lim_{\rho\to\infty}(f, g, \text{and } \psi)=0, \qquad \text{all } y, \tag{17}$$

$$\begin{aligned} \partial f/\partial\rho|_a &= [2+g(a,y)](2ZeQ/a\epsilon kT), && \text{for } |y|\leqslant L, \\ &=0, && \text{for } |y|>L, \end{aligned} \tag{18}$$

$$\begin{aligned} \partial g/\partial\rho|_a &= 2ZeQf(a,y)/a\epsilon kT, && \text{for } |y|\leqslant L, \\ &=0, && \text{for } |y|>L, \end{aligned} \tag{19}$$

$$\begin{aligned} \partial\psi/\partial\rho|_a &= -2ZeQ/a\epsilon kT, && \text{for } |y|\leqslant L, \\ &=0, && \text{for } |y|>L, \end{aligned} \tag{20}$$

where $a=\kappa a'$ and $L=\kappa L'$.

There are two approximations that can be applied at this point to simplify the equations. The most important is the familiar Debye–Hückel one. If we consider f, g, and ψ to be small, then we will retain only the lowest, nonzero order of magnitude terms in ZeQ/kT of eqs. (13)–(15). The second approximation is that this work is only concerned with Kerr region behavior, i.e. only those terms that result in a dipole energy strictly proportional to E^2 will be retained. Under these approximations, we can subdivide f, g, and ψ into those components that are symmetric about the cylinder axis and unperturbed by the field, ψ_+, f_+, and g_+, and those distortions that are an odd function of y and whose magnitude is proportional to E, f_- and g_-. In terms of these functions and the parameter ZeQ/kT, the lowest, nonzero order of magnitude terms for f_+, ψ_+ and g_- are proportional to ZeQ/kT, while for g_+ and f_- there are no linear terms, and only terms in the differential equations and boundary conditions proportional to $(ZeQ/kT)^2$ survive as the lowest, nonzero order of magnitude ones.

$$\begin{aligned} &\nabla^2 f_+ - f_+ = 0, \quad \lim_{\rho=\infty} f_+ = 0, \\ &\qquad \partial f_+/\partial\rho|_a = 4ZeQ/a\epsilon kT, \quad |y| \leqslant L, \\ &\qquad\qquad = 0, \quad |y| > L, \end{aligned} \tag{21}$$

$$\begin{aligned} &\nabla^2 g_+ = \tfrac{1}{2} f_+^2 - \nabla f_+ \cdot \nabla \psi_+, \quad \lim_{\rho\to\infty} g_+ = 0, \\ &\qquad \partial g_+/\partial\rho|_a = 2f_+(a,y) ZeQ/a\epsilon kT, \quad |y| \leqslant L, \\ &\qquad\qquad = 0, \quad |y| > L, \end{aligned} \tag{22}$$

$$\begin{aligned} &\nabla^2 \psi_+ = -\tfrac{1}{2} f_+, \quad \lim_{\rho\to\infty} \psi_+ = 0, \\ &\qquad \partial\psi_+/\partial\rho|_a = -2ZeQ/a\epsilon kT, \quad |y| \leqslant L, \\ &\qquad\qquad = 0, \quad |y| > L, \end{aligned} \tag{23}$$

$$\begin{aligned} &\nabla^2 g_- = E\, \partial f_+/\partial y, \quad \lim_{\rho\to\infty} g_- = 0, \\ &\qquad \partial g_-/\partial\rho|_a = 0, \quad \text{all } y, \end{aligned} \tag{24}$$

$$\begin{aligned} &\nabla^2 f_- - f_- = E\, \partial g_+/\partial y + \tfrac{1}{2} g_- f_+ - \nabla g_- \cdot \nabla \psi_+, \quad \lim_{\rho\to\infty} f_- = 0, \\ &\qquad \partial f_-/\partial\rho = \tfrac{1}{2} g_-(a,y)\, \partial f_+/\partial\rho|_a. \end{aligned} \tag{25}$$

Eqs. (21)–(23) are standard Debye–Hückel expressions for the ion atmosphere of a finite charged rod, in the absence of a field. If we expand the function f_+ as a cosine Fourier series on the y interval $[-C, +C]$, where C is taken arbitrarily large enough such that $f_+(\rho, C) \approx 0$, the solution of eq. (21) is

$$f_+ \frac{ALK_0(\rho)}{2aCK_1(a)} + \sum_{n=1}^{\infty} \frac{A \sin(\beta_n L) K_0(\lambda_n \rho)}{C\beta_n \lambda_n a K_1(\lambda_n a)} \cos(\beta_n y), \tag{26}$$

where $A = -8ZeQ/\epsilon kT$, $\beta_n = n\pi/C$, and $\lambda_n^2 = \beta_n^2 + 1$. $K_0(x)$ and $K_1(x)$ are modified Bessel functions of the second kind of orders 0 and 1.

It can be readily verified by substitution, that the solutions of eqs. (22) and (23) are given by

$$g_+(\rho, y) = \tfrac{1}{4} f_+^2(\rho, y), \tag{27}$$

$$\psi_+(\rho, y) = -\tfrac{1}{2} f_+(\rho, y). \tag{28}$$

That these are the standard Debye–Hückel solutions can be seen by expanding Boltzmann exponentials,

$$n_+ = n_0\, e^{-\psi} \approx n_0 (1 - \psi + \tfrac{1}{2}\psi^2), \qquad n_- = n_0\, e^{\psi} \approx n_0 (1 + \psi + \tfrac{1}{2}\psi^2).$$

In terms of this and eqs. (2) and (11)

$$f_+ = (n_+ - n_-)/n_0 = -2\psi, \qquad g_+ = (n_+ + n_- - 2n_0)/n_0 = \psi^2,$$

which are equivalent to eqs. (27) and (28).

Eq. (10) for the dipole moment, m, of the system is transformed in the ρ and y coordinate system to

$$m=\frac{2\pi ZEn_0}{\kappa^4}\int_{-\infty}^{+\infty} y\,\mathrm{d}y\int_a^{\infty}\rho\,\mathrm{d}\rho f_-(\rho,y). \tag{29}$$

In order to calculate this expression, it is not necessary to solve explicitly eq. (25) for f_-. In order to simplify the resulting expression, however, we take f_- to be of the form

$$f_-(\rho,y)=\tfrac{1}{4}f_+(\rho,y)g_-(\rho,y)+f'_-(\rho,y), \tag{30}$$

where $f'_-(\rho,y)$ satisfies

$$\nabla^2 f'_- - f'_- = \tfrac{1}{4}Ef_+\partial f_+/\partial y+\tfrac{1}{2}f_+g_-, \tag{31}$$

with $\lim_{\rho\to\infty} f'_- = 0$, and

$$\partial f'_-/\partial\rho|_a=\tfrac{1}{4}g_-(a,y)\,\partial f_+(a,y)/\partial\rho$$

where eqs. (21), (24), (25), (27) and (28) have been used.

Rearranging eq. (31), we have for f'_-,

$$f'_-(\rho,y)=\nabla^2 f'_- - \tfrac{1}{4}Ef_+\,\partial f_+/\partial y-\tfrac{1}{2}f_+g_-. \tag{32}$$

Substituting this into eq. (29), integrating ∇^2 by parts, with $\partial f'_-/\partial y\to 0$, as $|y|\to\infty$, yields

$$m=-\frac{\pi Zen_0}{2\kappa^4}\int_{-\infty}^{+\infty} y\,\mathrm{d}y\int_a^{\infty}\rho\,\mathrm{d}\rho f_+(g_-+E\,\partial f_+/\partial y)-\frac{\pi Zen_0 a}{2\kappa^4}\int_{-\infty}^{+\infty} y\,\mathrm{d}y g_-(a,y)\,\partial f_-(a,y)/\partial\rho. \tag{33}$$

It only remains, therefore, to solve eq. (24) for $g_-(\rho,y)$ in order to calculate the dipole moment. If we expand g_- as a sine Fourier series over the arbitrarily large y interval $\{-C,+C\}$, we obtain

$$g_-(\rho,y)=-\sum_{n=1}^{\infty}\frac{AE}{C}\sin(\beta_n L)\left(\frac{K_0(\lambda_n\rho)}{\lambda_n aK_1(\lambda_n a)}-\frac{K_0(\beta_n\rho)}{\beta_n aK_1(\beta_n a)}\right)\sin(\beta_n y), \tag{34}$$

where β_n, λ_n, and A are defined in eq. (26). Using this expression in eq. (33) and integrating, we find

$$m=(4\epsilon Z^2E'/\kappa^3)(e^2Q/\epsilon kT)^2F(a,L), \tag{35}$$

where

$$\begin{aligned}F(a,L)=\frac{2}{C}\sum_{n=1}^{\infty}\Bigg\{&(-1)^n\frac{L\sin(\beta_nL)}{4\beta_n}\Bigg[\left(\frac{K_0(\lambda_na)}{\lambda_naK_1(\lambda_na)}-\frac{K_0(\beta_na)}{\beta_naK_1(\beta_na)}\right)\\&+\frac{2}{\beta_n^2}\left(\frac{K_0(a)}{aK_1(a)}-\frac{K_0(\lambda_na)}{\lambda_naK_1(\lambda_na)}\right)-\frac{1}{1-\beta_n^2}\left(\frac{K_0(\beta_na)}{\beta_naK_1(\beta_na)}-\frac{K_0(a)}{aK_1(a)}\right)\Bigg]\\&+\frac{\sin^2(\beta_nL)}{8\beta_n^2}\left\{2\left(\frac{K_0(\beta_na)}{\lambda_naK_1(\lambda_na)}\right)+\frac{1}{2}\left[\frac{1}{\lambda_n^2}-\left(\frac{aK_0(\lambda_na)}{\lambda_naK_1(\lambda_na)}\right)^2\right]\right\}\\&+\sum_{\substack{m=1\\m\neq n}}^{\infty}(-1)^{n+m}\frac{\beta_n\sin(\beta_nL)\sin(\beta_mL)}{2\beta_m(\beta_n^2-\beta_m^2)}\Bigg[\left(\frac{K_0(\lambda_na)}{\lambda_naK_1(\lambda_na)}-\frac{K_0(\beta_na)}{\beta_naK_1(\beta_na)}\right)\\&+\frac{2}{\beta_n^2-\beta_m^2}\left(\frac{K_0(\lambda_ma)}{\lambda_maK_1(\lambda_ma)}-\frac{K_0(\lambda_na)}{\lambda_naK_1(\lambda_na)}\right)-\frac{1}{1+(\beta_n^2-\beta_m^2)}\left(\frac{K_0(\beta_na)}{\beta_naK_1(\beta_na)}-\frac{K_0(\lambda_ma)}{\lambda_maK_1(\lambda_ma)}\right)\Bigg]\Bigg\}.\end{aligned} \tag{36}$$

The inner double sum can be written in abbreviated form as

$$F(a,L)=\sum_{n=0}^{\infty}\sum_{\substack{m=0\\m\neq n}}^{\infty}(-1)^{n+m}F(\beta_n,\beta_m).$$

Taking advantage of the alternating signs, this can be expressed as

$$F(a,L)=\sum_{n=1}^{\infty}\sum_{i=1}^{\infty}\frac{[F(\beta_n,\beta_{n+2+2i})-F(\beta_n,\beta_{n+1+2i})]}{\beta_{n+2+2i}-\beta_{n+1+2i}}(\beta_{n+2+2i}-\beta_{n+1+2i})$$
$$+\sum_{m=1}^{\infty}\sum_{i=1}^{\infty}\frac{F(\beta_{m+2+2i},\beta_m)-F(\beta_{m+1+2i},\beta_m)}{\beta_{m+2+2i}-\beta_{m+1+2i}}(\beta_{m+2+2i}-\beta_{m+1+2i}).$$

Written in this manner, the inner sum can be expressed as the integral of a derivative or as

$$F(a,L)=\frac{1}{2}\sum_{n=1}^{\infty}\int_{\beta_{n+1}}^{\infty}\frac{\partial F(\beta_n,y)}{\partial y}\,\mathrm{d}y+\frac{1}{2}\sum_{m=1}^{\infty}\int_{\beta_{m+1}}^{\infty}\frac{\partial F(y,\beta_m)}{\partial y}\,\mathrm{d}y.$$

Integrating and retaining only those terms that will sum to a nonzero value for the dipole moment as $C\to\infty$ results in

$$F(a,L)=\frac{1}{C}\sum_{n=1}^{\infty}\left\{\frac{\sin(\beta_nL)\sin(\beta_{n+1}L)}{\beta_1\beta_n\beta_{n+1}}\left[-\left(\frac{2}{\beta_n+\beta_{n+1}}+\frac{(\beta_n+\beta_{n+1})(1+\beta_{n+1}\beta_1)}{1+\beta_1(\beta_{n+1}+\beta_n)}\right)\frac{K_0(\lambda_{n+1}a)}{\lambda_{n+1}aK_1(\lambda_{n+1}a)}\right.\right.$$
$$+\left(\frac{2}{\beta_n+\beta_{n+1}}+\frac{(\beta_n+\beta_{n+1})(1-\beta_1\beta_n)}{1-\beta_1(\beta_{n+1}+\beta_n)}\right)\frac{K_0(\lambda_na)}{\lambda_naK_1(\lambda_na)}$$
$$\left.\left.-\frac{\beta_1\beta_{n+1}(\beta_n+\beta_{n+1})}{1-\beta_1(\beta_n+\beta_{n+1})}\frac{K_0(\beta_{n+1}a)}{\beta_{n+1}aK_1(\beta_{n+1}a)}-\frac{\beta_1\beta_n(\beta_n+\beta_{n+1})}{1+\beta_1(\beta_n+\beta_{n+1})}\frac{K_0(\beta_na)}{\beta_naK_1(\beta_na)}\right]\right\}. \tag{37}$$

It is this equation that we use to calculate polarizabilities. For large values of C (e.g. ≈ 100 for $L=1$), $F(a,L)$ is independent of C. The terms of the sum begin to vanish rapidly once $\beta_nL>5$. For DNA, the factor containing the charge density, Q, takes on special significance. In the symbolism of Manning [7], this is just the effective reduced charge density of DNA, ξ_{net}, as determined by counterion condensation. It is related to the charge of the counterion, Z, in the condensed layer by,

$$\xi_{\mathrm{net}}=1/Z. \tag{38}$$

Since the polarizability along the rod, $\alpha_{\parallel}$, is defined by m/E', we can write

$$\alpha_{\parallel}=\epsilon F(a,L)/\kappa^3. \tag{39}$$

It is perhaps reasonable at this point to attempt to interpret qualitatively the equations. A good discussion has already been given by Stigter [12] in connection with the electrophoretic velocity of charged rods oriented parallel to an electric field. Eqs. (24) and (25) will result in nonzero solutions for f_- and g_- only if $\partial f_+/\partial y\neq 0$. In other words, an excess or deficit of ion atmosphere charge will accumulate at those points where there already exists a charge concentration gradient in the direction of the field. The formation of a steady-state ion atmosphere flow rests basically on the establishment of a charge density equilibrium between the undirectional force due to the applied field and the electric force due to the charge on the central rod. The latter force, proportional to $-\partial\psi_+/\partial x$, or, in the Debye–Hückel approximation, to $\frac{1}{2}\,\partial f_+/\partial x$, is an odd function about the origin, always in the direction of the rod (see fig. 1). For a finite, charged rod, $\partial f_+/\partial x$ is a maximum at the ends, decreasing rapidly due to ion atmosphere shielding and cancellations of x-direction forces from different parts of the rod, until it vanishes at the origin. For practical purposes, $\partial f_+/\partial x$ is significant for only a few Debye lengths [(3–4)/κ] from the ends. Ion atmosphere polarization is, therefore, primarily an end effect, and as such should increase at a significantly slower rate than the L^3 dependence predicted by the condensed counterion polarization model for DNA [8,9]. For DNA rods that are much longer than the Debye length, it is not difficult to predict a linear length dependence for the polarizability.

3. Results and discussion

In the limiting case of a very thin rod, i.e. $a \ll 1$, we can use the approximations that for $x \ll 1$, $K_0(x) \approx -\ln x$ and $x\,K_1(x) \approx 1$. In this limit, the function $F(a,L)$ [eq. (36)] is independent of a. A plot of $\ln F(L)$ as a function of $\ln L$ is shown in fig. 2. As can be observed, for $L \leqslant 6$, $F(L)$ is approximately proportional to $L^{1.85}$. Recalling the definition of L from eq. (36) and substituting into eq. (39), we find that

$$\alpha_{\parallel} = \text{const.}(L')^{1.85}/\kappa^{1.15}, \tag{40}$$

where L' is the half length of the rod. This can be compared with the experimental results of Hogan et al. [2], who find an L^2/κ dependence for the polarizability. It should be mentioned, however, that whereas they observed linear dependence of the orientation on field strength, our treatment of the ion atmosphere polarization results in a classical E^2 dependence, at low enough field strengths. Our own experiments [1,13] indicate that the orientation is consistent with an E^2 dependence at low fields. Our experiments also indicate that the polarizability is an inverse function of κ. For $L > 6$, the ends of the rod become increasingly isolated, electrostatically, and the power dependence of $F(L)$ on L slowly approaches 1, as expected. In this limit, the polarizability, as a function of L' and κ is

$$\alpha_{\parallel} = \text{const.}\ L'/\kappa^2. \tag{41}$$

Of experimental significance in assessing the contribution of ion atmosphere polarization is the dependence of α in eq. (39) on counterion charge, in particular, with the effective charge density of the rod, Q. That the dipole moment is proportional to Q^2 is not surprising in that one power of Q comes from the linear dependence of the electrostatic force due to the rod, $-\partial\psi/\partial x$, on Q, while another power of Q is a result of the linear dependence of the total charge in the ion atmosphere with charge density. For a highly charged polyelectrolyte as DNA, the effective charge density can be manipulated by varying the charge of the

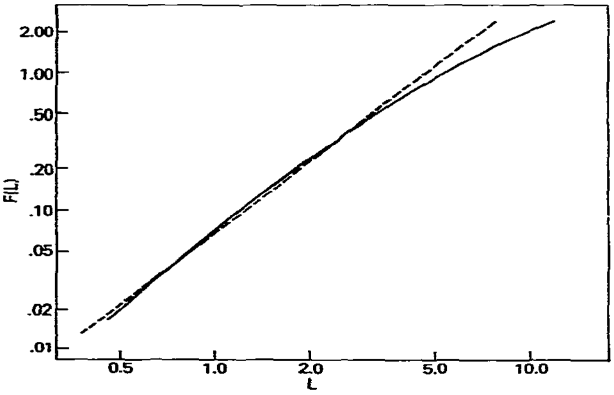

Fig. 2. The solid line shows the dependence of the function $F(L)$ on L. The dashed line shows the best fitting straight line to the curve for $L \leqslant 6$. The slope of this line is used in determining the power dependence of the polarizability with rod length L' and ionic strength.

counterion. As shown by eq. (39), however, the effects of counterion charge on effective charge density and the interaction with the electric field cancel. This is the experimental result reported by Hogan et al. [2] and Charney et al. [9]. The same prediction is made, however, for the polarization of the condensed counterions [8,9] and so is not a good test of the importance of the ion atmosphere contribution. One possible test is the change in polarizability in mixed Na^+–Mg^{2+} systems. Eqs. (53) and (54) of ref. [7] give a method of calculating effective charge densities in mixed counterion systems. If we take as an example a Na^+ concentration of 250 μM, then the charge density will increase ≈40% (from 0.76 to 0.83 charge neutralization) with a free Mg^{2+} concentration of less than 20 μM. It is then possible to significantly alter the charge density of DNA without equally distorting the charge composition of the ion atmosphere.

A quantitative comparison of theory and experiment is the subject of another paper [13]. A specific example, however, will serve as an indication of ion atmosphere importance. If we take a DNA length of 800 Å ($=2L'$), a Debye length of 200 Å ($1/\kappa$), and use the effective DNA charge density for Na^+ from counterion condensation theory [7], a polarizability of $\alpha_{\parallel} = 6.4 \times 10^{-16}$ cm^3 can be calculated from eqs. (37) and (39). This can be compared with our experimentally observed value of $\approx 8 \times 10^{-16}$ cm^3. For these same conditions, we can calculate a predicted polarizability for the condensed counterions (eqs. (27) of ref. [8]) of $\alpha_{\parallel} = 3.7 \times 10^{-16}$ cm^3. Our experimental evidence indicates that both polarizations are contributing to the orientation at this ionic strength and DNA length.

Although the equations in this paper have been derived specifically for a rigid rod of uniform charge density, it should not prove difficult to extend the treatment to other structures, in the Debye–Hückel limit. The functions f_+, g_+, ψ_+, and g_- can be determined through the appropriate summation of the equivalent functions for small spheres. In this way, more complicated structures can be constructed in much the same fashion as has been done for hydrodynamic calculations [15]. As was done here, the dipole moment can be calculated directly from these functions if an appropriate analogue for the boundary conditions for $\partial f_-(a,y)/\partial \rho$ is constructed.

It is possible, however, to investigate qualitatively the expected differences between a random coil and a rigid rod. If we consider the random coil to be equivalent to an elastic, porous, charged sphere, an important difference with the rigid rod model is that the coil charge density in the direction of the field is gaussian rather than constant. In contrast to rigid rod behavior, therefore, ion atmosphere polarization is not expected to be an end effect for random coils, but rather will extend throughout the polymer domain. Furthermore, as the viscoelastic coil stretches in the field, the average charge density in the direction of the field will decrease. This could well be the origin of the hypopolarizability inferred by Rau and Bloomfield [14] from the relative relaxation times for the rise and decay processes. Initial calculations indicate that this effect would be of the correct magnitude to account for their results (work in progress).

Although it is not unreasonable at low field strengths to consider the ion atmosphere separately from the condensed counterions, the same will not hold true at high fields. In light of the recent discussions concerning the relationship between counterion condensation and a full Poisson–Boltzmann treatment of the ion atmosphere [16–18], it would seem reasonable to expect that a steady-state flow treatment with full Poisson–Boltzmann equations, i.e. not with the Debye–Hückel approximation, would be instructive in considering the saturation problems of the dipole moment of DNA at high fields.

4. Conclusions

We have developed an expression for the induced dipole energy resulting from the polarization of the ion atmosphere surrounding a charged rod, with a particular emphasis on explaining the polarizability of DNA. The results have been shown to be in qualitative agreement with experimental results. In a paper that is in preparation we shall demonstrate experimentally that at least a component of the polarizability of rod-like DNA fragments is in quantitative agreement with the equations presented here.

References

[1] E. Charney and K. Yamaoka, XXIII Intern. Congr. Pure and appl. chem., Preprint Vol. 1 (Boston, 1971) p. 252.
[2] M. Hogan, N. Dattagupta and D.M. Crothers, Proc. Natl. Acad. Sci. USA 75 (1978) 195.
[3] S. Takashima, Biopolymers 5 (1967) 899.
[4] J.P. McTague and J.H. Gibbs, J. Chem. Phys. 44 (1966) 4295.
[5] F. van der Touw and M. Mandel, Biophys. Chem. 2 (1974) 218.
[6] K. Kikuchi and K. Yoshioka, Biopolymers 15 (1976) 583.
[7] G.S. Manning, Quart. Rev. Biophys. 11 (1978) 179.
[8] G.S. Manning, Biophys. Chem. 9 (1978) 65.
[9] E. Charney, K. Yamaoka and G.S. Manning, Biophys. Chem. 11 (1980) 167.
[10] D. Stigter, J. Phys. Chem. 82 (1978) 1417.
[11] P.H. Wiersema, A.L. Loeb and J.Th.G. Overbeek, J. Colloid Interface Sci. 22 (1966) 78.
[12] D. Stigter, J. Phys. Chem. 82 (1978) 1424.
[13] D.C. Rau and E. Charney, in preparation.
[14] D.C. Rau and V.A. Bloomfield, Biopolymers 18 (1979) 2783.
[15] J. Garcia de la Torre and V.A. Bloomfield, Biopolymers 16 (1977) 1747.
[16] J.A. Schellman and D. Stigter, Biopolymers 16 (1977) 1415.
[17] M. Fixman, J. Chem. Phys. 70 (1979) 4995.
[18] R.W. Wilson, D.C. Rau and V.A. Bloomfield, Biophys. J. 30 (1980) 317.